

Video Article

Simultaneous Recordings of Cortical Local Field Potentials and Electrocorticograms in Response to Nociceptive Laser Stimuli from Freely Moving Rats

Lupeng Yue^{1,2}, Fengrui Zhang³, Xuejing Lu^{1,2}, You Wan^{4,5,6}, Li Hu^{1,2}

¹CAS Key Laboratory of Mental Health, Institute of Psychology, University of Chinese Academy of Sciences

²Department of Psychology, University of Chinese Academy of Sciences

³Research Center of Brain Cognitive Neuroscience, Liaoning Normal University

⁴Neuroscience Research Institute, Peking University

⁵Department of Neurobiology, School of Basic Medical Sciences, Peking University

⁶Key Laboratory for Neuroscience, Ministry of Education/National Health and Family Planning Commission, Peking University

Correspondence to: You Wan at ywan@hsc.pku.edu.cn, Li Hu at huli@psych.ac.cn

URL: <https://www.jove.com/video/58686>

DOI: [doi:10.3791/58686](https://doi.org/10.3791/58686)

Keywords: Electroencephalogram (EEG), electrocorticogram (ECoG), local field potential (LFP), laser-evoked potential (LEP), pain, animal model, simultaneous recording

Date Published: 12/24/2018

Citation: Yue, L., Zhang, F., Lu, X., Wan, Y., Hu, L. Simultaneous Recordings of Cortical Local Field Potentials and Electrocorticograms in Response to Nociceptive Laser Stimuli from Freely Moving Rats. *J. Vis. Exp.* (), e58686, doi:10.3791/58686 (2018).

Abstract

Electrocortical responses, elicited by laser heat pulses that selectively activate nociceptive free nerve endings, are widely used in many animal and human studies to investigate the cortical processing of nociceptive information. These laser-evoked brain potentials (LEPs) consist of several transient responses that are time-locked to the onset of laser stimuli. However, the functional properties of the LEP responses are still largely unknown, due to the lack of a sampling technique that can simultaneously record neural activities at the surface of the cortex (*i.e.*, electrocorticogram [ECoG] and scalp electroencephalogram [scalp EEG]) and inside the brain (*i.e.*, local field potential [LFP]). To address this issue, we present here an animal protocol using freely moving rats. This protocol is composed of three main procedures: (1) animal preparation and surgical procedures, (2) a simultaneous recording of ECoG and LFP in response to nociceptive laser stimuli, and (3) data analysis and feature extraction. Specifically, with the help of a 3D-printed protective shell, both ECoG and LFP electrodes implanted on the rat's skull were securely held together. During data collection, laser pulses were delivered on the rat's forepaws through gaps in the bottom of the chamber when the animal was in spontaneous stillness. Ongoing white noise was played to avoid the activation of the auditory system by the laser-generated ultrasounds. As a consequence, only nociceptive responses were selectively recorded. Using the standard analytical procedures (*e.g.*, band-pass filtering, epoch extraction, and baseline correction) to extract stimulus-related brain responses, we obtained results showing that LEPs with a high signal-to-noise ratio were simultaneously recorded from ECoG and LFP electrodes. This methodology makes the simultaneous recording of ECoG and LFP activities possible, which provides a bridge of electrocortical signals at the mesoscopic and macroscopic levels, thereby facilitating the investigation of nociceptive information processing in the brain.

Video Link

The video component of this article can be found at <https://www.jove.com/video/58686/>

Introduction

EEG is a technique to record electrical potentials and oscillatory brain activities generated by the synchronized activities of thousands of neurons in the brain. It is popularly used in many basic studies and clinical applications^{1,2}. For instance, EEG responses to intense laser heat pulses (*i.e.*, LEPs) are widely adopted to investigate the peripheral and central processing of nociceptive sensory input^{3,4,5}. In humans, LEPs mainly consist of three distinct deflections: the early component (N1) that is somatotopically organized and likely to reflect the activity of the primary somatosensory cortex (S1)⁶, and the late components (N2 and P2) that are centrally distributed and more likely to reflect the activity of bilateral generators in the secondary somatosensory cortex, insula, and anterior cingulate cortex^{7,8}. In previous studies^{9,10}, we demonstrated that rat LEPs, sampled using ECoG (a type of intracranial EEG) from electrodes placed directly on the exposed surface of the brain, also consist of three distinct deflections (*i.e.*, somatotopically organized N1 and the centrally distributed N2 and P2). The polarity, order, and topography of the rat LEP components are similar to human LEPs¹¹. However, due to the limited spatial resolution of the scalp EEG and subdural ECoG recordings¹², as well as the inaccurate nature of EEG source analysis techniques¹³, the detailed contribution of the neural activities to the LEP components is much debated. For example, it is unclear if and the extent to which S1 contributes to the early part of the cortical response (N1) elicited by laser stimuli⁶.

Different from the recording technique at the macroscopic level, direct intracranial recordings using microwire arrays aided by a stereotaxic apparatus and microdrives^{14,15} could measure neural activities (*e.g.*, LFPs) of specific regions. LFPs mainly reflect the summation of inhibitory

or excitatory postsynaptic potentials of local neuronal populations¹⁶. Since LFP-sampled neural activities reflect neuronal processes occurring within hundreds of micrometers around the recording electrode, this recording technique is widely used to investigate the information processing in the brain at the mesoscopic level. However, it only focuses on precise local changes of brain activities and cannot answer the question of how signals from multiple regions are integrated (e.g., how LEP components are integrated at multiple brain regions).

It is worth noting that the simultaneous recording of an ECoG and cortical LFPs from freely moving rats could facilitate the investigation of cortical information processing at both macroscopic and mesoscopic levels. In addition, this methodology provides an excellent opportunity to investigate the extent to which the neural activities of the predefined brain regions contribute to the LEPs. Indeed, several previous studies have assessed the coherence between spikes, cortical LFP, and ECoG signals^{17,18} and demonstrated that the LFP^{19,20} adjacent to the EEG electrode contributes to the formation of stimulus-related brain responses. However, the existing technique is usually used to record brain responses from anesthetized animals due to the lacking of a protective shell to prevent the electrodes from being damaged by the collision. In other words, the technique that could build the bridge of electrocortical signals at the mesoscopic (cortical LFP) and macroscopic (EEG and ECoG) levels in freely moving rats is still lacking.

To address this issue, we developed a technique that could record an ECoG and cortical LFPs in multiple brain regions simultaneously from freely moving rats. This technique helps establish the direct relationship of electrocortical signals at the mesoscopic and macroscopic levels, thus facilitating the investigation of nociceptive information processing in the brain.

Protocol

Adult male Sprague-Dawley rats (weighing 400 - 450 g) were used in the experiment. All surgical and experimental procedures followed the Guide for Care and Use of Laboratory Animals of the National Institutes of Health. The procedures were approved by the Research Ethics Committee at the Institute of Psychology, Chinese Academy of Sciences.

1. Electrode Implantation

1. Anesthetize the rat in a chamber with 5% isoflurane and an air flow rate of 1 L/min before the surgery.
2. Using a stereotaxic apparatus, fix the head of the rat with its nose placed into the anesthetic mask. Administrate isoflurane *via* the anesthetic mask at a concentration of 2% with an air flow rate of 0.5 L/min to maintain the anesthetic depth during the surgery. Note that the surgical tolerance is achieved when the rat fails to respond to toe-pinching.
3. Apply ophthalmic ointment to the eyes to avoid corneal drying.
4. Shave the top of the rat scalp using a standard shaver.
5. Sterilize the scalp using the medical iodophor disinfectant solution and 75% alcohol to remove the iodine.
6. Inject lidocaine (2%) into the scalp for local analgesia. Administer atropine (0.2 mL i.p.) to inhibit respiratory hypersecretion.
7. Make a midline incision of approximately 2 - 3 cm on the scalp using a scalpel. Cut and remove part of the scalp along the midline and expose the cranium. Use the electrocoagulator to stop the bleeding, when necessary.
8. Mark the locations of ECoG electrodes based on the predefined stereotaxic coordinates (placed according to the position of Bregma) and the locations of the reference and ground electrodes on the midline (placed 2 and 4 mm caudally to the Lambda, respectively).
9. Drill holes (diameter: 0.5 mm) for the ECoG screws, using an electric cranial drill on the skull at the marked sites, without destroying the dura.
10. Drive a stainless-steel screw (outside diameter: 0.6 mm), which connects to the insulation-coated copper wire, into the hole for approximately 1 mm depth without penetrating the underlying dura. These screws act as ECoG, reference, and ground electrodes during the experiment.
11. Place a protective shell base on the cranium. Fix the base with its adjacent screws on the cranium using dental acrylic. Use medical cotton that could be removed afterward to protect the area that is intended to be used for depth wire implantation from being covered.
NOTE: The protective shell is a custom-designed 3D-printed polylactic product, which consists of three parts: a base, a wall, and a cap. The wall is covered by copper tapers to construct as a Faraday cage.
12. Mark the locations of the depth wire electrodes based on the predefined stereotaxic coordinates.
13. Drill small holes (diameter: 0.2 mm) on the skull around the marked sites for wire implantation, and carefully remove the bone flap to expose the dura. Wash the craniotomy frequently, using normal saline. **Figure 1** describes the set-up before the implantation of the depth wire electrodes.
14. Using a needle, lift and cut the dura without damaging the pia mater, vessels, and the surface of the neocortex.
15. Lower the depth wire electrodes to the surface of the neocortex and, then, slowly penetrate the brain to the target depth. Frequently stop moving down the electrodes for cortical resilience. In the present study, the depth of the wire tip is 0.5 mm under the cortical surface.
16. Seal the craniotomy with a mixture of wax and paraffin oil to ensure that the depth wire electrodes can be moved for subsequent experimental manipulations.
17. Fix the electrode apparatus using dental acrylic on the skull.
18. Weld each copper wire that connects to the ECoG screw to the corresponding channel on the connector module. Cover the welding spots using clay to avoid potential contact between different channels.
19. Assemble the protective shell wall to the base and weld the reference and ground electrodes to the corresponding channels.
20. Fix the cap to the protective shell using tapes to avoid contamination.
21. Inject the rat with penicillin (60,000 U, i.p.) immediately after surgery to prevent postsurgical infections.
22. Single-house the rat in a temperature- and humidity-controlled cage and keep it in a 12-h day/night cycle after the surgery, with food and water *ad libitum* for at least one week prior to the LEP experiment.
NOTE: To simultaneously record ECoG and cortical LFP activities, an apparatus was used here that was assembled with two types of electrodes linked to a connector module, which contained several microdrives attached to the tungsten wire arrays. The gold pins were used to connect the tungsten wires to the electrode interface board (EIB) of the connector module by pressing the wires into small metal holes on the EIB. Two metal holes on the EIB were soldered with coated copper wires, and the open end of each copper wire was soldered with the corresponding copper wire connected to ECoG screw. The details of fabrication have been described elsewhere²¹.

2. Data Collection

1. Tickle the rat at least 1x a day for three or more consecutive days before the experiment to ensure that the rat gets familiar with the experimenter²².
2. Place the rat in the behavior chamber for at least 1 h before the experiment to ensure the rat acclimatizes to the recording environment.
NOTE: The chamber is a plastic cube with a side length of 30 cm. The bottom of the chamber is made of an iron grating with ~8 mm gaps.
3. Connect the recording headstage with the electrode module gently, to avoid scaring the rat and damaging the electrode module.
4. Set up the laser generator, connect the optic fiber, and adjust the spot size of the laser according to the equipment operator's manual.
Connect the digital output from the trigger generator to the digital input port of the recording board.
NOTE: Take care not to curl the optic fiber excessively to avoid breaking off the fiber. Before recording, make sure the trigger signals are displayed and recorded by the recording software. In this protocol, radiant-heat stimuli are generated by an infrared neodymium yttrium aluminum perovskite (Nd: YAP) laser with a wavelength of 1.34 μm . The diameter of the laser spot size is set at approximately 5 mm by focusing lenses. A He-Ne laser pointed to the stimulated area, which is defined depending on the objective of the experiment. Also, the stimulus energy of the laser pulses is determined according to the experimental design. The laser pulse duration is 4 ms.
5. Set the video camera beneath the corner of the experimental chamber to continuously record the nociceptive behaviors of the rat when its paw receives nociceptive laser stimuli. Adjust the position and direction of the camera to make sure the nociceptive behaviors are completely recorded throughout the experiment.
NOTE: A high-speed charge-coupled device (CCD) camera is highly recommended, as it can deliver the operating signals to the main board of the recording system to record the onset time and duration of the nociceptive behavior precisely. Nociceptive behaviors are assessed by the experimenter after each laser stimulus, according to previously defined criteria based on the animal movement^{23,24}, as follows: no movement (score = 0), head-turning (including shaking or elevating the head; score = 1), flinching (*i.e.*, a small abrupt body jerking movement; score = 2), withdrawal (*i.e.*, paw retraction from the laser stimulus; score = 3), licking and whole-body movement (score = 4).
6. Deliver ongoing white noise (50 dB SPL) via a loudspeaker at the top of the chamber.
NOTE: As shown in previous studies^{10,25}, laser stimulation delivered on the skin generates ultrasounds that can be detected by the rat auditory system. For this reason, ongoing white noise is played throughout the experiment to avoid the activation of the auditory system in response to laser-generated ultrasounds. This procedure allows the selective recording of brain responses related to the activation of the nociceptive system.
7. Collect the electrophysiological data from both the ECoG and the depth wire electrodes, using the recording system according to the equipment operator's manual.
NOTE: The operating signals of the camera and the trigger signals of the laser pulses are sampled simultaneously with the electrophysiological data at the same sampling rate (all data are amplified and digitized using a sampling rate of 20,000 Hz), which ensures that all data are time-synchronized.
8. Deliver the laser pulses to the plantar of the rat's forepaw through the gaps in the bottom of the chamber.
NOTE: The laser stimulus is only delivered when the rat is spontaneous stillness for more than 2 s based on the experimenter's observation, to minimize the signal contamination of the movement-related artifacts. To avoid nociceptor fatigue or sensitization, the target of the laser beam is displaced manually after each stimulus, and the interstimulus interval is never shorter than 40 s. ECoG and LFP signals can be recorded several times from each rat. The rat needs to be put in the experimental chamber 1 h before each recording session. After all recording sessions, the rat was deeply anesthetized and perfused transcardially with ice-cold phosphate-buffered saline followed by 4% paraformaldehyde. The brain was removed from the skull and sectioned to identify the electrode positions.

3. Data Analysis

1. Filter the continuous data with a band-pass filter between 1 and 30 Hz.
2. Epoch the data using an analysis window of 3 s, extended from 1 s before to 2 s after the onset of laser stimuli. Baseline correction is performed by subtracting the mean amplitude within the prestimulus interval.
3. Manually reject the epochs that are contaminated by gross artifacts.
4. Compute the averaged LEP waveforms and time lock to the onset of laser stimuli for each experimental condition.
5. Compute the wavelet transform coherence (WTC) of LEP waveforms recorded from ECoGs and depth wire electrodes.
NOTE: WTC is a technique to perform the coherence between pairs of electrodes as a function of time and frequency. The WTC between two signals can be calculated for any time-frequency point, which has the advantage of generating coherence values for the entire time-frequency spectrum. The details of the methodology have been described elsewhere²⁶.

Representative Results

In the representative experiment, the electrophysiological data from five rats were recorded. The laser stimuli were delivered to the right forepaw of each rat for 20 times with 40 s interstimulus intervals. The laser-evoked brain responses were recorded using both ECoG screws and depth wires, and the depth wires were implanted in bilateral primary somatosensory cortices (S1) and primary motor cortices (M1).

As summarized in **Figure 1**, two ECoGs (marked in black) and depth wire electrodes (marked in color, five wires for each of the four regions) were placed according to stereotaxic coordinates in the following positions (expressed in reference to the Bregma, in mm; positive X and Y axis values indicate right and anterior locations, respectively): in the left ECoG, X = -1.5 and Y = 1.75; in the right ECoG, X = 1.5 and Y = 1.75; in the left S1, X = -4 and Y = 0.5; in the right S1, X = 4 and Y = 0.5; in the left M1, X = -3 and Y = 3; in the right M1, X = 3 and Y = 3.

Figure 2 shows the raw electrophysiological data from all electrodes (two ECoG screws plus four by five tungsten wires, five tungsten wires in each brain region), with the onset of laser stimulus marked by a vertical dot line. Please note that clear LEP responses are detectable after the onset of the laser stimulus.

Figure 3 shows the group-level-averaged LEP waveforms from six electrodes (two ECoG screws plus four tungsten wires, a representative tungsten wire in each brain region) of five rats. Regardless of the recording site, the LEP responses consist of a dominant negative deflection (N1 wave). The latency and amplitude of the N1 wave are as follows (mean \pm SEM): for the left ECoG, 143 ± 9 ms and -51 ± 4 μ V; for the right ECoG, 145 ± 9 ms and -47 ± 4 μ V; for the left S1, 149 ± 9 ms and -86 ± 7 μ V; for the right S1, 168 ± 10 ms and -71 ± 6 μ V; for the left M1, 179 ± 12 ms and -74 ± 7 μ V; for the right M1, 185 ± 11 ms and -63 ± 6 μ V. Importantly, N1 latencies in the bilateral ECoG and LFP signals recorded from the contralateral S1 are similar, which are clearly shorter than those recorded from the ipsilateral S1 and bilateral M1. In contrast, N1 amplitudes are largest in contralateral S1 and smallest in bilateral ECoGs.

Figure 4 shows the WTC between LEPs sampled using the ECoG screws (the signals from two ECoG screws were averaged) and depth wires at different brain regions (right M1, right S1, left M1, and left S1). Note that the contralateral (left) S1 and M1 showed a higher coherence than the ipsilateral (right) S1 and M1 at the gamma-frequency band (50 - 100 Hz).

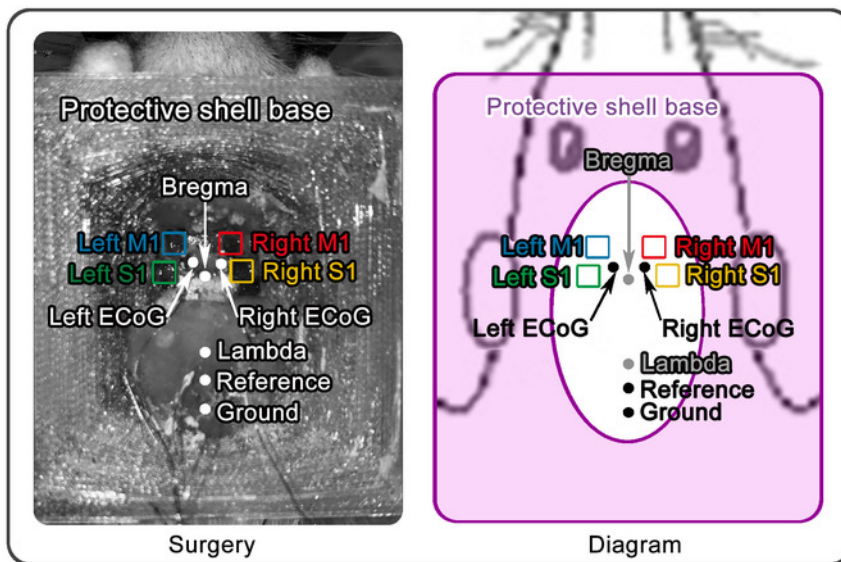


Figure 1: Electrode implantation set-up. Before the implantation of the depth wire electrodes, a protective shell base is placed on the cranium, and the screws used as ECoG electrodes are driven into the predefined holes and fixed by dental acrylic. Four holes are drilled for the implantation of depth wire electrodes (e.g., tungsten wire arrays) at the positions. These positions are at the top of the left and right S1 and M1, respectively. The screws used as reference and ground electrodes are placed 2 and 4 mm caudally to the Lambda and fixed with the protective shell base. The panel on the left shows the photo of surgery after the implantation of a protective shell base. The panel on the right shows the diagram of surgery, which showed the general shape of the protective shell base. [Please click here to view a larger version of this figure.](#)

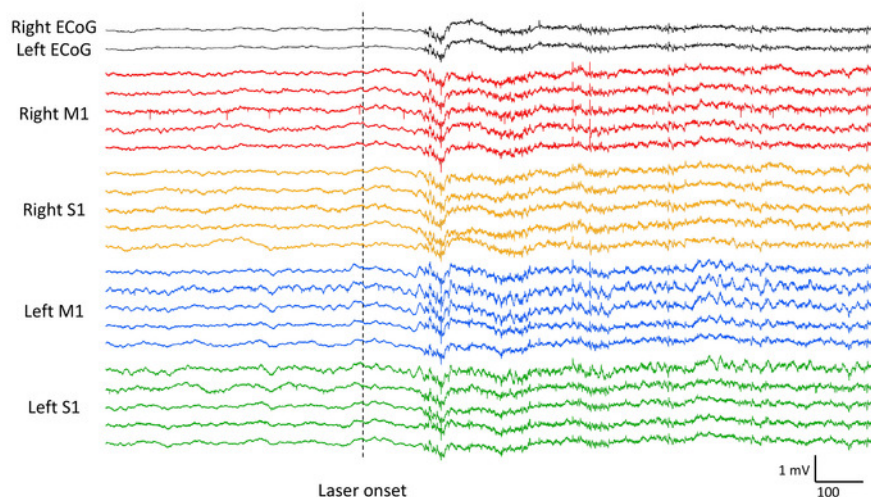


Figure 2: Raw electrophysiological data of a representative rat. Displayed signals are recorded from a representative rat with two ECoGs and 20 depth wire electrodes (five electrodes in each brain region), using the electrode located 2 mm caudally to the Lambda as reference. The onset of the laser stimulus is marked using a vertical dot line. [Please click here to view a larger version of this figure.](#)

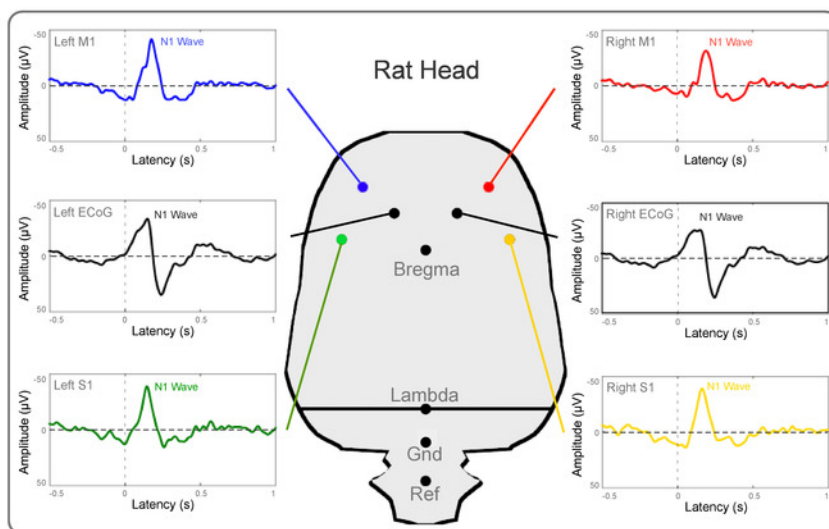


Figure 3: Group-level-averaged LEP waveforms. The displayed averaged signals are recorded from five rats at two ECoGs and four depth wire electrodes (one representative electrode in each brain region), using the electrode located 2 mm caudally to the Lambda as reference. [Please click here to view a larger version of this figure.](#)

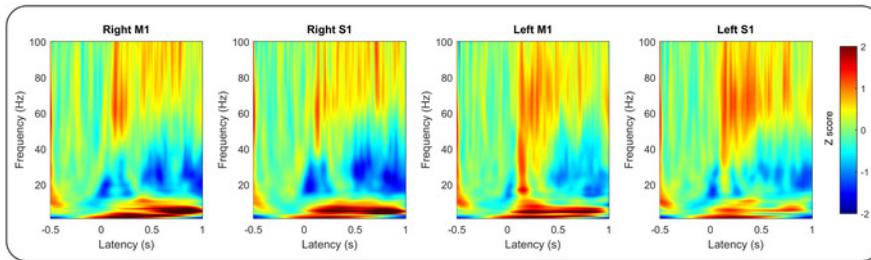


Figure 4: The wavelet transform coherence. The displayed results show the wavelet transform coherence between LEPs sampled using ECoG screws and depth wires at different brain regions (right M1, right S1, left M1, and left S1). The coherence was normalized to the respective baseline (0.5 s before the laser stimulus onset). [Please click here to view a larger version of this figure.](#)

Discussion

In the present study, we described a technique to concurrently record ECoGs and cortical LFP responses elicited by nociceptive laser stimuli from freely moving rats. The results showed that LEP responses could be clearly detected after the onset of laser stimuli in both ECoG and LFP signals. The successful simultaneous recording of ECoG and cortical LFP signals will enable scientists to investigate their relationship for better understanding the contribution of neuronal activities to the LEP components.

Five critical steps in the proposed technique should be noted. First, it is important to make sure that the surface of the cranium is clean and dry before fixing the protective shell base on it, using dental acrylic. This step enables that the protective shell base is stably fixed. Second, since the diameter of the ECoG screws is slightly larger than that of the holes, the initial screw driving will enlarge the hole to form the screw-thread. In the present study, the distance between the hole for tungsten wires and the hole for the ECoG screw is very small (e.g., less than 0.3 mm). If all holes are drilled before the ECoG screw driving and depth wire insertion, the skull around the ECoG holes would be fragile, and it would not bear the mechanical load of the hole enlargement during the screw driving. For this reason, the ECoG screws need to be driven into the holes to form the screw-thread prior to the hole drilling for the tungsten wire insertion. If the inserted ECoG screws obstruct the view when drilling the holes for the tungsten wires, it is recommended they are to be driven out and driven in again after step 1.14 of the protocol. Third, when inserting the depth wire electrodes, the experimenter is supposed to pay attention to the resistance at the tip of the tungsten wires, which usually indicates that the depth wires are blocked by the hole edge on the skull or the dura when that has not been completely removed. If this is the case, the depth wires must be raised, and the possible obstacles should be cleaned out before reinserting the electrodes²⁰. Fourth, when filling the craniotomy holes with the mixture of wax and paraffin oil after the electrode implantation, the implanted wires should not be touched. Therefore, it is preferable to melt the nearby-placed mixture using electrocoagulator. Fifth, it is important to ensure that the distance between the laser end piece and the target site on the rat is kept at approximately 1 cm to guarantee that the perceived laser energies are consistent among different trials^{10,25}.

Indeed, to make sure that the protective shell can cover and protect the whole apparatus, the size of the shell is designed to be relatively large (a cube with a side length of 3.5 mm) compared to the rat's head. To minimize the influence of the over-the-head device on the rat's movement, we recommend using rats who weighed more than 400 g in the experiment. For this reason, this technique cannot be used to study sophisticated behaviors in the rat model and should not be adopted in other models of smaller animals (e.g., mice), even though the proposed technique can be combined with other techniques and extended to many other applications. For example, this technique can be easily applied to record brain responses evoked by stimuli of different sensations (e.g., auditory and visual)^{27,28} and applied in identifying brain features of psychiatric diseases (e.g., epilepsy)²⁹ in freely moving rats, which would promote the investigation of their respective neural mechanisms. In addition, the electrode implantation can withstand the test for about one month, which provides the possibility to perform a longitudinal study in the future.

Altogether, we provide a valid technique to simultaneously record ECoG and LFP activities from freely moving rats. This technique enables us to investigate the information processing in the brain at both mesoscopic and macroscopic levels. This is important for translational studies to document experimental animal findings for a better understanding of human physiology and pathophysiology.

Disclosures

The authors have nothing to declare.

Acknowledgements

This work was supported by CAS Key Laboratory of Mental Health, Institute of Psychology, the National Natural Science Foundation of China (31471082, 31671141, and 31822025 to L.H.), the 13th Five-year Informatization Plan of the Chinese Academy of Sciences (XXH13506 to L.H.), the Scientific Foundation project of the Institute of Psychology, Chinese Academy of Sciences (Y6CX021008 to L.H.).

References

1. Klimesch, W., Doppelmayr, M., Schwaiger, J., Winkler, T., Gruber, W. Theta oscillations and the ERP old/new effect: independent phenomena? *Clinical Neurophysiology*. **111** (5), 781-793 (2000).
2. Peng, W. *et al.* Brain oscillations reflecting pain-related behavior in freely moving rats. *Pain*. **159** (1), 106-118 (2018).

3. Treede, R. D. Neurophysiological studies of pain pathways in peripheral and central nervous system disorders. *Journal of Neurology*. **250** (10), 1152-1161 (2003).
4. Iannetti, G. D. *et al.* Evidence of a specific spinal pathway for the sense of warmth in humans. *Journal of Neurophysiology*. **89** (1), 562-570 (2003).
5. Bromm, B., Treede, R. D. Nerve fibre discharges, cerebral potentials and sensations induced by CO₂ laser stimulation. *Human Neurobiology*. **3** (1), 33-40 (1984).
6. Valentini, E. *et al.* The primary somatosensory cortex largely contributes to the early part of the cortical response elicited by nociceptive stimuli. *NeuroImage*. **59** (2), 1571-1581 (2012).
7. Valeriani, M. *et al.* Parallel spinal pathways generate the middle-latency N1 and the late P2 components of the laser evoked potentials. *Clinical Neurophysiology*. **118** (5), 1097-1104 (2007).
8. Kuo, C. C., Yen, C. T. Comparison of anterior cingulate and primary somatosensory neuronal responses to noxious laser-heat stimuli in conscious, behaving rats. *Journal of Neurophysiology*. **94** (3), 1825-1836 (2005).
9. Hu, L. *et al.* The primary somatosensory cortex and the insula contribute differently to the processing of transient and sustained nociceptive and non-nociceptive somatosensory inputs. *Human Brain Mapping*. **36** (11), 4346-4360 (2015).
10. Xia, X. L., Peng, W. W., Iannetti, G. D., Hu, L. Laser-evoked cortical responses in freely-moving rats reflect the activation of C-fibre afferent pathways. *NeuroImage*. **128**, 209-217 (2016).
11. Jin, Q. Q. *et al.* Somatotopic Representation of Second Pain in the Primary Somatosensory Cortex of Humans and Rodents. *The Journal of Neuroscience*. **38** (24), 5538-5550 (2018).
12. Lenkov, D. N., Volnova, A. B., Pope, A. R., Tsytarev, V. Advantages and limitations of brain imaging methods in the research of absence epilepsy in humans and animal models. *Journal of Neuroscience Methods*. **212** (2), 195-202 (2013).
13. Mouraux, A., Iannetti, G. D. Across-trial averaging of event-related EEG responses and beyond. *Magnetic Resonance Imaging*. **26** (7), 1041-1054 (2008).
14. Li, X. *et al.* Extracting Neural Oscillation Signatures of Laser-Induced Nociception in Pain-Related Regions in Rats. *Frontiers in Neural Circuits*. **11**, 71 (2017).
15. Zhao, Z. F., Li, X. Z., Wan, Y. Mapping the Information Trace in Local Field Potentials by a Computational Method of Two-Dimensional Time-Shifting Synchronization Likelihood Based on Graphic Processing Unit Acceleration. *Neuroscience Bulletin*. **33** (6), 653-663 (2017).
16. Buzsaki, G., Anastassiou, C. A., Koch, C. The origin of extracellular fields and currents--EEG, ECoG, LFP and spikes. *Nature Reviews Neuroscience*. **13** (6), 407-420 (2012).
17. Bimbi, M. *et al.* Simultaneous scalp recorded EEG and local field potentials from monkey ventral premotor cortex during action observation and execution reveals the contribution of mirror and motor neurons to the mu-rhythm. *NeuroImage*. **175**, 22-31 (2018).
18. Musall, S., von Pfostl, V., Rauch, A., Logothetis, N. K., Whittingstall, K. Effects of neural synchrony on surface EEG. *Cerebral Cortex*. **24** (4), 1045-1053 (2014).
19. Bruyns-Haylett, M. *et al.* The neurogenesis of P1 and N1: A concurrent EEG/LFP study. *NeuroImage*. **146**, 575-588 (2017).
20. Kang, S., Bruyns-Haylett, M., Hayashi, Y., Zheng, Y. Concurrent Recording of Co-localized Electroencephalography and Local Field Potential in Rodent. *Journal of Visualized Experiments*. (129), e56447 (2017).
21. Shikano, Y., Sasaki, T., Ikegaya, Y. Simultaneous Recordings of Cortical Local Field Potentials, Electrocardiogram, Electromyogram, and Breathing Rhythm from a Freely Moving Rat. *Journal of Visualized Experiments*. (134), e56980 (2018).
22. Cloutier, S., LaFollette, M. R., Gaskill, B. N., Panksepp, J., Newberry, R. C. Tickling, a Technique for Inducing Positive Affect When Handling Rats. *Journal of Visualized Experiments*. (135), e57190 (2018).
23. Fan, R. J., Kung, J. C., Olausson, B. A., Shyu, B. C. Nocifensive behaviors components evoked by brief laser pulses are mediated by C fibers. *Physiology & Behavior*. **98** (1-2), 108-117 (2009).
24. Fan, R. J., Shyu, B. C., Hsiao, S. Analysis of nocifensive behavior induced in rats by CO₂ laser pulse stimulation. *Physiology & Behavior*. **57** (6), 1131-1137 (1995).
25. Hu, L. *et al.* Was it a pain or a sound? Across-species variability in sensory sensitivity. *Pain*. **156** (12), 2449-2457 (2015).
26. Catarino, A. *et al.* Task-related functional connectivity in autism spectrum conditions: an EEG study using wavelet transform coherence. *Molecular Autism*. **4** (1), 1 (2013).
27. Polterovich, A., Jankowski, M. M., Nelken, I. Deviance sensitivity in the auditory cortex of freely moving rats. *PLoS One*. **13** (6), e0197678 (2018).
28. Li, G., Baker, C. L., Functional organization of envelope-responsive neurons in early visual cortex: organization of carrier tuning properties. *The Journal of Neuroscience*. **32** (22), 7538-7549 (2012).
29. Fujita, S., Toyoda, I., Thamattoor, A. K., Buckmaster, P. S. Preictal activity of subicular, CA1, and dentate gyrus principal neurons in the dorsal hippocampus before spontaneous seizures in a rat model of temporal lobe epilepsy. *The Journal of Neuroscience*. **34** (50), 16671-16687 (2014).